

# A mixed finite element method for nonlinear and nearly incompressible elasticity based on biorthogonal systems

Bishnu P. Lamichhane\*

*Centre for Mathematics and its Applications, Mathematical Sciences Institute, Australian National University, ACT 0200, Canberra*

## SUMMARY

We present a finite element method for nonlinear and nearly incompressible elasticity. The formulation is based on Petrov–Galerkin discretization for the pressure and is closely related to the average nodal pressure formulation presented earlier in the context of incompressible and nearly incompressible dynamic explicit applications [1]. Some numerical examples are presented to show the efficiency of the approach. Copyright © 2000 John Wiley & Sons, Ltd.

KEY WORDS: Mixed finite elements, displacement–based formulation, Petrov–Galerkin discretization, biorthogonal system

*AMS Subject Classification: 65N30, 65N15, 74B10*

## 1. Introduction

As linear, bilinear or trilinear finite elements based on the standard displacement–based formulation of elasticity exhibit a poor performance when applied to the nearly incompressible case, it is essential either to work with higher order finite elements or introduce an additional unknown leading to a mixed formulation. Among some popular methods is the method of enhanced assumed strain, which was first proposed by SIMO AND RIFAI in [2]. The enhanced assumed strain is also extended to nonlinear elasticity, see, e.g., [3, 4, 5]. The mathematical analysis of the enhanced assumed strain for linear elasticity has been done in [6, 7, 8]. In particular, a uniform convergence of finite element approximation in the nearly incompressible case is established. The method of enhanced assumed strain is derived by using the Hu–Washizu principle [9, 10]. Another important method called mixed enhanced strain has been introduced by KASPER AND TAYLOR [11, 12] for linear and nonlinear elasticity by using the Hu–Washizu principle as the point of departure. The extension of the mixed enhanced formulation to simplicial meshes is done in [13] using the idea of mini-element formulation requiring that the pressure variable is continuous. Thus it introduces an additional number of unknowns and static condensation of the pressure variable is not easy.

---

\*Correspondence to: Centre for Mathematics and its Applications, Mathematical Sciences Institute, Australian National University, ACT 0200, Canberra, [Bishnu.Lamichhane@maths.anu.edu.au](mailto:Bishnu.Lamichhane@maths.anu.edu.au)

In the analysis of the linear Hu–Washizu formulation in the discrete setting, it is required that the space of displacement and the trace space of the discrete spherical part of the space of stress satisfy a uniform inf-sup condition with a constant independent of meshsize and the Lamé parameter  $\lambda$  [7, 8]. The analysis is restricted to quadrilateral and hexahedral meshes, where a subspace of the trace space of the discrete spherical part of the space of stress can be constructed which satisfies a uniform inf-sup condition with the space of displacement. Hence the mathematical analysis is quite restrictive and does not cover even general quadrilateral and hexahedral meshes. Due to instability, these approaches cannot be applied to a nearly incompressible elastic problem with a simplicial mesh. Even using quadrilateral or hexahedral meshes, although the numerical results for the displacement are quite promising in the linear and nonlinear case, spurious pressure modes can appear in the pressure or the volumetric part of the stress [7].

Although the linear Hu–Washizu formulation is uniform among different papers, there are some variants of nonlinear Hu–Washizu formulation. For example, in the nonlinear Hu–Washizu formulation considered in [2, 12], the displacement, the first Piola–Kirchhoff stress tensor and the deformation gradient are regarded as independent variables. Different Hu–Washizu functionals are considered in [14, 15]. Another three-field formulation based on the displacement, the deformation gradient and the Kirchhoff stress is considered in [16] to alleviate locking in nonlinear elasticity.

It is quite standard to use a mixed formulation depending on displacement and pressure for nearly incompressible elasticity in simplicial meshes [17, 18]. However, the mixed formulation requires an inf-sup stable pair for the displacement and pressure, and working with discontinuous pressure, higher order finite elements should be used. On the other hand, the finite element discretization leads to a saddle point system requiring a special type of solver. The mixed displacement–pressure formulation including the B-bar method can be easily generalized to nonlinear setting [14, 19, 15]. The method yields promising numerical results with bilinear or trilinear basis functions for the displacement and piecewise constant functions for the pressure working with quadrilateral or hexahedral meshes. However, for linear finite elements based on simplicial meshes, it has not been found any discretization based on discontinuous pressure which allows easy static condensation of the pressure variable.

In this paper, we consider a generalization of the discretization scheme based on enforcing a constant pressure field over a patch of triangles or tetrahedra [1, 20, 21, 22, 23]. The method of enforcing a constant pressure field over a patch of triangles or tetrahedra has originally been introduced in [1] for incompressible and nearly incompressible dynamic explicit applications and is called average nodal pressure formulation. Similar ideas have been exploited in [20, 21, 22, 23, 24] to deal with nonlinear and nearly incompressible elasticity in simplicial meshes. The idea of using average nodal pressure formulation can be traced back to finite volume schemes, where control volumes are built by using a finite element mesh [25, 26]. Combining the idea of finite volume element method with the mixed finite element method, the average nodal pressure formulation for linear elasticity is analyzed in [27] under the framework of mixed finite elements. We have shown that the method presented in [1] can be written as a Galerkin mixed formulation using primal and dual meshes, where the trial and test functions for the pressure variable are piecewise constant functions on the dual mesh. As the method originally considered in [1] does not satisfy a uniform inf-sup condition, we propose to enrich the displacement field with bubble functions [27], which leads to a stable formulation. Since pressure variable is discretized using piecewise constant functions on the dual mesh,

the mass matrix for the pressure equation is diagonal. If we do not enrich the displacement field with bubble functions and statically condense out the pressure variable from the system, the approach based on primal and dual meshes [27] reduces to the average nodal pressure formulation considered in [1]. In [27], we have also presented another approach based on the same displacement field but using primal and dual bases instead of primal and dual meshes. As the mass matrix for the pressure equation is exactly the same for both approaches, and the second approach is more easily generalized to the higher order case than the first approach, we think of this approach as the generalization of the approach based on primal and dual meshes.

Here we extend the second approach to nonlinear hyperelasticity, which gives rise to a nonlinear mixed formulation. The main motivation to consider the second approach is that it is not so easy to use a numerical integration in the first approach as the discrete variational formulation of this approach is based on primal and dual meshes.

The mixed formulation is obtained by introducing a pressure-like variable as an additional unknown. Although the formulation can easily be generalized to any hyperelastic material law, we present the formulation specifically for Mooney–Rivlin material law, which includes neo-Hookean material law as a special case [28]. We use standard linear finite elements to discretize the displacement variable whereas a Petrov–Galerkin discretization is employed to discretize the pressure variable. The trial and test spaces are different for the pressure equation leading to a non-symmetric formulation. The basis functions of the trial space are standard linear finite element basis functions, whereas the basis functions of the test space are constructed in such a way that the basis functions of the trial and test spaces satisfy a biorthogonality relation. The biorthogonality relation is a very important ingredient of our formulation as it gives rise to a diagonal mass matrix and enables us to statically condense out the pressure variable from the nonlinear saddle point system matrix. As a result, we arrive at a displacement–based formulation. Then the standard Newton method can be applied to solve the discrete displacement–based nonlinear equation. Although due to the Petrov–Galerkin discretization of the pressure equation, the displacement–based formulation is not symmetric, the system matrix is sparse. Therefore, an iterative solver for non-symmetric system can be used to solve the arising linear system [29, 30]. If we use an exact solver, it is evident that the new approach is more efficient than the standard mini-element approach. However, we do not compare the efficiency of this approach with the mini-element approach in terms of solver. If a neighboring search algorithm is used when assembling the stiffness matrix, the degree of freedom corresponding to pressure variable can already be eliminated during assembling process.

We note that the mathematical analysis for the mixed formulation based on primal and dual meshes uses the stability of the mini-element to prove inf-sup condition [27]. As a similar argument is necessary to show the uniform inf-sup condition in the formulation based on primal and dual bases [31], we need to enrich the space of displacement with element-wise defined bubble functions. The approach is suitable for simplicial as well as quadrilateral meshes as the dual basis can be locally constructed yielding a diagonal mass matrix for all these meshes [32]. However, at least three internal degree of freedom should be added to achieve stability in case of quadrilateral meshes [33]. In this paper, we restrict ourselves to the simplicial case.

The structure of the rest of the paper is organized as follows. In the next section, we briefly recall the standard and a mixed formulation of linear elasticity. The discrete formulation using different trial and test spaces is presented in Section 3, where the explicit construction of the test spaces are also provided. In Section 4, we present some selective numerical results in two

and three dimensions which demonstrate the efficiency of the approach.

## 2. Boundary value problem of hyperelasticity

This section is devoted to the introduction of the boundary value problem of hyperelasticity. We consider a homogeneous isotropic hyperelastic material body occupying a bounded domain  $\Omega$  in  $\mathbb{R}^d$ ,  $d = \{2, 3\}$  with polygonal or polyhedral boundary. Let  $\mathbf{x} \in \bar{\Omega}$  be a position vector of a point in the continuum body relative to the standard basis in  $\mathbb{R}^d$ . When the material body is deformed, the position vector  $\mathbf{x}$  of the material point is transformed to another point  $\tilde{\mathbf{x}}$  by means of a single-valued continuously differentiable mapping  $\phi : \Omega \rightarrow \mathbb{R}^d$ . The relation between this mapping and the displacement field  $\mathbf{u} : \Omega \rightarrow \mathbb{R}^d$  is given by

$$\tilde{\mathbf{x}} = \phi(\mathbf{x}) = \mathbf{x} + \mathbf{u}(\mathbf{x}). \quad (1)$$

The deformation gradient  $\mathbf{F}$  and the Jacobian of the deformation are defined by  $\mathbf{F} = \nabla \phi$  and  $J = \det \mathbf{F}$ . We assume that  $J > 0$  and  $\mathbf{F} = (F_{i,j})_{i,j=1}^d$  so that  $F_{i,j} \in L^2(\Omega)$ ,  $1 \leq i, j \leq d$ , where  $L^2(\Omega)$  denotes the space of square integrable functions in  $\Omega$ .

For a prescribed body force  $\mathbf{f} \in L^2(\Omega)^d$ , the governing equilibrium equation in  $\Omega$  reads

$$-\operatorname{div} \boldsymbol{\pi} = \mathbf{f}, \quad (2)$$

where  $\boldsymbol{\pi}$  is the first Piola-Kirchhoff stress tensor.

We assume that the material is hyperelastic and isotropic so that a stored energy function  $W$  exists with  $\boldsymbol{\sigma} = 2 \frac{\partial W(\mathbf{C})}{\partial \mathbf{C}}$ , where  $\boldsymbol{\sigma}$  is the second Piola-Kirchhoff stress tensor, and  $\mathbf{C}$  is the right Cauchy-Green strain tensor given by  $\mathbf{C} = \mathbf{F}^T \mathbf{F}$ . Since we do not take the right Cauchy-Green strain tensor and the deformation gradient as independent variables, we assume that they are functions of displacement.

The boundary  $\partial\Omega$  is decomposed into  $\Gamma_N$  and  $\Gamma_D$  with  $\partial\Omega = \Gamma_N \cup \Gamma_D$  so that the displacement is assumed to satisfy homogeneous Dirichlet boundary condition on  $\Gamma_D$  and traction boundary condition on  $\Gamma_N$ .

The energy function  $W$  depends on the right Cauchy-Green strain tensor and hence from it on the deformation gradient. The first Piola-Kirchhoff tensor  $\boldsymbol{\pi}$  is related to the second Piola-Kirchhoff tensor  $\boldsymbol{\sigma}$  by  $\boldsymbol{\pi} = \mathbf{F} \boldsymbol{\sigma}$ . Defining  $\tilde{W}(\mathbf{F}) := W(\mathbf{C})$ , we can write  $\boldsymbol{\pi} = \frac{\partial \tilde{W}(\mathbf{F})}{\partial \mathbf{F}}$ . For the isotropic material the energy function  $W$  depends only on the three principal invariants  $I_C$ ,  $II_C$  and  $III_C$  of  $\mathbf{C}$ , where  $I_C = \operatorname{tr}(\mathbf{C})$ ,  $II_C = \frac{1}{2}(\operatorname{tr}^2(\mathbf{C}) - \operatorname{tr}(\mathbf{C}^2))$ , and  $III_C = \det(\mathbf{C}) = J^2$  with  $J := \det(\mathbf{F})$ . If the material law satisfies the two-term Mooney-Rivlin law [28], we have

$$\begin{aligned} W(\mathbf{C}) &= \lambda U(J) + \frac{\mu}{2} [(1 - c_m)(I_C - 3 - 2 \ln(J)) + c_m(II_C - 3 - 2 \ln(J))] , \\ \boldsymbol{\sigma} &= \lambda U'(J) J \mathbf{C}^{-1} + \mu [(1 - c_m)(\mathbf{1} - \mathbf{C}^{-1}) + c_m(\operatorname{tr} \mathbf{C} \mathbf{1} - \mathbf{C} - \mathbf{C}^{-1})] , \end{aligned}$$

where  $\lambda$  and  $\mu$  are Lamé parameters and  $0 \leq c_m \leq 1$  is a material constant. The real-valued function  $U$  is given by  $U(J) = \frac{1}{4}(J^2 - 1 - 2 \ln J)$ . We recall that the standard neo-Hookean law is recovered when  $c_m = 0$ .

In order to write the variational formulation of the problem, we introduce a Sobolev space  $\mathbf{V} := \{\mathbf{u} \in (W^{1,r}(\Omega))^d : \mathbf{u}|_{\Gamma_D} = 0\}$  with a suitable  $r \geq 2$ , see [34]. The Sobolev space  $W^{1,r}(\Omega)$  for  $r \in \mathbb{N}$  is a Banach space and is equipped with the norm  $\|\cdot\|_{W^{1,r}(\Omega)}$  [35]. By using the

Banach space  $L^r(\Omega)$  having the  $L^r$ -norm defined as

$$\|v\|_{L^r(\Omega)} := \left( \int_{\Omega} |v|^r dx \right)^{1/r}, \quad v \in L^r(\Omega),$$

we can define the  $W^{1,r}$ -norm  $\|\cdot\|_{W^{1,r}(\Omega)}$  as

$$\|v\|_{W^{1,r}(\Omega)} := \left( \|v\|_{L^r(\Omega)}^r + \sum_{k=1}^d \left\| \frac{\partial v}{\partial x_k} \right\|_{L^r(\Omega)}^r \right)^{1/r}, \quad v \in W^{1,r}(\Omega).$$

Hence the Sobolev space  $W^{1,r}(\Omega)$  is defined in a standard way,

$$W^{1,r}(\Omega) := \{v \in L^1_{loc}(\Omega) : \|v\|_{W^{1,r}(\Omega)} < \infty\}.$$

Let  $\mathbf{n}$  be the normal vector on the boundary of  $\Omega$  written as column vector. We assume that the material body occupying the region  $\Omega$  satisfies the traction boundary condition on  $\Gamma_N$  as

$$\boldsymbol{\pi} \mathbf{n} = \mathbf{g}_N. \tag{3}$$

Now the standard variational formulation of the nonlinear elasticity problem is written as: find  $\mathbf{u} \in \mathbf{V}$  so that

$$\int_{\Omega} \boldsymbol{\pi} : \nabla \mathbf{v} dx = \int_{\Omega} \mathbf{f} \cdot \mathbf{v} dx + \int_{\Gamma_N} \mathbf{g}_N \cdot \mathbf{v} d\sigma, \quad \mathbf{v} \in \mathbf{V}. \tag{4}$$

**Mixed formulation** When a material is nearly incompressible, the Lamé parameter  $\lambda \rightarrow \infty$  and the determinant of the Jacobian of transformation  $J \rightarrow 1$ . The main drawback of linear, bilinear or trilinear finite elements in the standard displacement-based formulation is that when the determinant of the Jacobian is constrained to be close to 1, the displacement is vanishingly small, and this is called volumetric locking. Here, we relax this constraint by introducing a pressure-like variable  $p = \lambda U'(J)J$ . A similar pressure-like variable is introduced in [36] to study the convergence of finite element approximations of the nonlinear elasticity problems in the incompressible limit. We note that there is no restriction in introducing a pressure variable different from the one that we have introduced as far as the variable is an  $L^2$ -function. Writing a variational equation for  $p$ , our variational formulation reads: given a body force  $\mathbf{f} : \Omega \rightarrow \mathbb{R}^d$  and a traction vector  $\mathbf{g}_N : \Gamma_N \rightarrow \mathbb{R}^d$ , find  $(\mathbf{u}, p) \in \mathbf{V} \times L^2(\Omega)$  such that

$$\begin{aligned} \int_{\Omega} (\mathbf{F}^{-T}(\mathbf{u})p + G(\mathbf{u})) : \nabla \mathbf{v} dx &= \int_{\Omega} \mathbf{f} \cdot \mathbf{v} dx + \int_{\Gamma_N} \mathbf{g}_N \cdot \mathbf{v} d\sigma, & \mathbf{v} \in \mathbf{V}, \\ \int_{\Omega} (p - \lambda U'(J(\mathbf{u}))J(\mathbf{u}))q dx &= 0, & q \in L^2(\Omega), \end{aligned} \tag{5}$$

where  $G(\mathbf{u}) = \mu \left[ (1 - c_m) \left( \mathbf{F}(\mathbf{u}) - \mathbf{F}(\mathbf{u})^{-T} \right) + c_m \left( \text{tr} C(\mathbf{u}) \mathbf{F}(\mathbf{u}) - \mathbf{F}(\mathbf{u}) C(\mathbf{u}) - \mathbf{F}(\mathbf{u})^{-T} \right) \right]$ , and  $\mathbf{F}(\mathbf{u})^{-T}$  is the inverse of  $\mathbf{F}(\mathbf{u})^T$ .

### 3. Discrete setting

We consider a locally quasi-uniform triangulation  $\mathcal{T}_h$  consisting of simplices of the domain  $\Omega$ . Let  $S_h$  be the space of linear finite elements defined on the triangulation  $\mathcal{T}_h$ ,

$$S_h := \{v_h \in C^0(\Omega) : v_h|_T \in \mathcal{P}_1(T), T \in \mathcal{T}_h\},$$

where  $\mathcal{P}_1(T)$  is the space of linear polynomials on  $T$ .

Defining the space of bubble functions

$$B_h := \{b_T \in C^0(T) : b_T|_{\partial T} = 0, \text{ and } \int_T b_T dx > 0, T \in \mathcal{T}_h\},$$

we introduce our finite element space for the displacement as  $\mathbf{V}_h^B := (S_h \oplus B_h)^d \cap \mathbf{V}$ , see [37, 17, 38]. Here, we use the standard cubic bubble function for  $b_T$  in our computation [38]. The motivation to discretize the displacement using the space  $\mathbf{V}_h^B$  comes from the fact that the pair  $(\mathbf{V}_h^B, S_h)$  satisfies a uniform inf-sup condition in case of linear elasticity, see [27, 31].

As mentioned in the introduction, we employ Petrov–Galerkin discretization for the variational equation of the pressure. The trial space for the pressure equation is  $S_h$ , whereas the basis functions in the test space are constructed in a special way. Let the space of the standard linear finite element functions  $S_h$  be spanned by the basis  $\{\phi_1, \dots, \phi_N\}$ . Now, we construct a dual basis  $M_h$  spanned by the basis  $\{\mu_1, \dots, \mu_N\}$  so that the basis functions of  $S_h$  and  $M_h$  satisfy a condition of biorthogonality relation

$$\int_{\Omega} \mu_i \phi_j dx = c_j \delta_{ij}, \quad c_j \neq 0, \quad 1 \leq i, j \leq n, \quad (6)$$

where  $N := \dim M_h = \dim S_h$ ,  $\delta_{ij}$  is the Kronecker symbol, and  $c_j$  a scaling factor. This scaling factor  $c_j$  can be chosen as proportional to the area  $|\text{supp}\phi_j|$ . It is easy to show that a local basis on the reference element  $\hat{T}$  can be easily constructed so that the equation (6) holds. Explicitly, for the reference triangle  $\hat{T} := \{(x, y) : 0 \leq x, 0 \leq y, x + y \leq 1\}$ , we have

$$\hat{\mu}_1 := 3 - 4x - 4y, \quad \hat{\mu}_2 := 4x - 1, \quad \text{and} \quad \hat{\mu}_3 := 4y - 1,$$

and for the reference tetrahedron  $\hat{T} := \{(x, y, z) : 0 \leq x, 0 \leq y, 0 \leq z, x + y + z \leq 1\}$ , we have

$$\hat{\mu}_1 := 4 - 5x - 5y - 5z, \quad \hat{\mu}_2 := 5x - 1, \quad \text{and} \quad \hat{\mu}_3 := 5y - 1, \quad \hat{\mu}_4 := 5z - 1.$$

The global basis functions for the test space are constructed by glueing the local basis functions together which is exactly the same procedure of constructing global finite element basis functions from the local ones. These global basis functions then satisfy the condition of biorthogonality (6) with global finite element basis functions, and  $\text{supp}\phi_i = \text{supp}\mu_i$ ,  $1 \leq i \leq n$ .

Thus, the finite element approximation of (5) is defined as a solution to the following problem: find  $(\mathbf{u}_h, p_h) \in \mathbf{V}_h^B \times S_h$  such that

$$\begin{aligned} \int_{\Omega} (\mathbf{F}^{-T}(\mathbf{u}_h)p_h + G(\mathbf{u}_h)) : \nabla \mathbf{v}_h d\mathbf{x} &= \int_{\Omega} \mathbf{f} \cdot \mathbf{v}_h d\mathbf{x} + \int_{\Gamma_N} \mathbf{g}_N \cdot \mathbf{v}_h d\sigma, & \mathbf{v}_h \in \mathbf{V}_h^B \\ \int_{\Omega} (p_h - \lambda U'(J(\mathbf{u}_h))J(\mathbf{u}_h))q_h d\mathbf{x} &= 0, & q_h \in M_h. \end{aligned} \quad (7)$$

We point out that the trial space for the pressure is spanned by the continuous linear finite element basis functions, whereas the test functions are not continuous. However, the test functions are defined exactly in the same way as the finite element basis functions, and the approach is conforming as  $M_h \subset L^2(\Omega)$ . Since  $\sum_{i=1}^{d+1} \hat{\mu}_i = 1$ , it is easy to prove that the space  $M_h$  contains constant functions, see also [32].

**Remark 1.** *If we use trial and test functions from the same space  $S_h$ , we arrive at a Galerkin mixed formulation and is equivalent to the so-called mini-element considered in [39] for the Stokes problem. This mixed finite element scheme satisfies the inf-sup condition for the linear elastic case and will be used to compare the performance of our approach in numerical experiments.*

In order to show that the pressure is approximated in an optimal way, we introduce a quasi-projection operator:  $Q_h : L^2(\Omega) \rightarrow S_h$ , which is defined as

$$\int_{\Omega} Q_h v \mu_h dx = \int_{\Omega} v \mu_h dx, \quad v \in L^2(\Omega), \mu_h \in M_h.$$

It is easy to verify that  $Q_h$  is well-defined and is identity if restricted to  $S_h$ . Hence,  $Q_h$  is a projection onto the space  $S_h$ . We note that  $Q_h$  is not the orthogonal projection onto  $S_h$  but an oblique projection onto it. Oblique projectors are studied extensively in [40], and different proofs on an identity on the norm of oblique projections are provided in [41].

This type of operator is introduced in [42] in the context of interpolation of non-smooth functions, and this operator is used in [43] in the context of mortar finite elements. The definition of  $Q_h$  allows us to write the discrete pressure as

$$p_h = \lambda Q_h(U'(J(\mathbf{u}_h))J(\mathbf{u}_h)). \tag{8}$$

Hence, it is sufficient to analyze the approximation property of the operator  $Q_h$  in the  $L^2$ -norm. Since  $S_h$  and  $M_h$  form a biorthogonal system, we can write  $Q_h$  as

$$Q_h v = \sum_{i=1}^n \frac{\int_{\Omega} \mu_i v dx}{c_i} \phi_i. \tag{9}$$

By using the above representation, we can show that  $Q_h$  is stable in the  $L^2$ -norm.

**Lemma 2.** For an arbitrary element  $T' \in \mathcal{T}_h$ , defining the closure of  $S_{T'}$  as

$$\bar{S}_{T'} = \bigcup \{ \bar{T} \in \mathcal{T}_h : \partial T \cap \partial T' \neq \emptyset \},$$

it holds

$$\|Q_h v\|_{L^2(T')} \leq C \|v\|_{L^2(\bar{S}_{T'})}, \quad v \in L^2(\Omega),$$

where the closure is indicated by the bar over the set. Hence

$$\|Q_h v\|_{L^2(\Omega)} \leq C \|v\|_{L^2(\Omega)}. \tag{10}$$

**Proof** Using the definition of  $Q_h$  as given in (9), we have

$$\|Q_h v\|_{L^2(T')} = \left\| \sum_{\substack{1 \leq i \leq n \\ T' \subset \text{supp} \phi_i}} \frac{\int_{\Omega} \mu_i v dx}{c_i} \phi_i \right\|_{L^2(T')}.$$

Since  $\text{supp} \phi_i = \text{supp} \mu_i$  for  $1 \leq i \leq n$ , we have

$$\int_{\Omega} \mu_i v dx = \int_{\text{supp} \phi_i} \mu_i v dx.$$

Denoting the support of  $\phi_i$  by  $S_i$  and applying the Cauchy–Schwarz inequality lead to

$$\left| \int_{S_i} \mu_i v dx \right| \leq \|\mu_i\|_{L^2(S_i)} \|v\|_{L^2(S_i)}$$

so that

$$\|Q_h v\|_{L^2(T')} \leq \sum_{\substack{1 \leq i \leq n \\ T' \subset S_i}} \frac{\|\mu_i\|_{L^2(S_i)} \|v\|_{L^2(S_i)}}{c_i} \|\phi_i\|_{L^2(T')}.$$

Since  $c_i$  is proportional to the area  $|S_i|$ , we estimate the  $L^2$ -norm by the  $L^\infty$ -norm and use the local quasi-uniformity to obtain

$$\|\mu_i\|_{L^2(S_i)} \|\phi_i\|_{L^2(T')} \leq C c_i,$$

where  $C$  is independent of the mesh-size. Thus

$$\|Q_h v\|_{L^2(T')} \leq C \sum_{\substack{1 \leq i \leq n \\ T' \subset S_i}} \|v\|_{L^2(S_i)}.$$

Noting that element  $T'$  is fixed and summation is restricted to those  $i$ 's with  $T' \subset S_i$ , we have

$$\|Q_h v\|_{L^2(T')} \leq C \|v\|_{L^2(S'_T)}.$$

The  $L^2$ -stability (10) then follows by summing this estimate over all elements  $T' \in \mathcal{T}_h$ .

The following lemma establishes the approximation property of the operator  $Q_h$  for a function  $v \in W^{s,2}(\Omega)$ . We note that the space  $W^{s,2}(\Omega)$  is a Hilbert space, which is usually denoted as  $H^s(\Omega)$ , and is defined similarly as the space  $W^{1,r}(\Omega)$ , see [35, 44].

**Lemma 3.** *For a function  $v \in W^{s,2}(\Omega)$ ,  $0 < s \leq 2$ , there exists a constant  $C$  independent of the mesh  $\mathcal{T}_h$  so that*

$$\|v - Q_h v\|_{L^2(\Omega)} \leq C h^s \|v\|_{W^{s,2}(\Omega)}.$$

**Proof** Let  $P_h : L^2(\Omega) \rightarrow S_h$  be the orthogonal projection onto  $S_h$  in  $L^2$ -sense. Using a triangle inequality, we obtain

$$\|v - Q_h v\|_{L^2(\Omega)} \leq \|v - P_h v\|_{L^2(\Omega)} + \|P_h v - Q_h v\|_{L^2(\Omega)}.$$

Since  $Q_h$  acts as an identity on  $S_h$ , we have

$$\|v - Q_h v\|_{L^2(\Omega)} \leq \|v - P_h v\|_{L^2(\Omega)} + \|Q_h(P_h v - v)\|_{L^2(\Omega)}.$$

Now we use the equation (10) to get

$$\|v - Q_h v\|_{L^2(\Omega)} \leq C \|v - P_h v\|_{L^2(\Omega)}.$$

Finally, the result follows by using the approximation property of the orthogonal projection  $P_h$  onto  $S_h$ , see [17, 18].

**Remark 4.** *Denoting the nodal solution vector of the pressure variable by  $\mathbf{p} = (p_1, \dots, p_N)^T$ , the discrete variational equation for the pressure is written as*

$$D\mathbf{p} = \mathbf{r}, \tag{11}$$

where  $D$  is a diagonal matrix because of the biorthogonality relation (6) and  $\mathbf{r}$  is a vector having  $i$ th component as

$$r_i = \lambda \int_{S_i} U'(J(\mathbf{u}_h)) J(\mathbf{u}_h) \mu_i d\mathbf{x},$$

where  $S_i$  is the support of the basis function  $\mu_i$  or  $\phi_i$ . Hence operator  $Q_h$  acts locally, and it is easy to compute  $Q_h \mu$  for any function  $\mu \in L^2(\Omega)$ . The elimination of the degree of freedom of the pressure variable is done by inverting the diagonal matrix  $D$ .

**Remark 5.** *If we redefine the function  $\mu_i$  to be the characteristic function at the  $i$ th node of the dual element, the pressure equation (11) is exactly the same as the one obtained by using primal and dual meshes [1, 27]. We note that  $J(\mathbf{u}_h)$  is not constant over a triangle as the displacement field is enriched with bubble functions. Therefore, an appropriate quadrature rule should be used to compute the linearized stiffness matrix.*

Observing Remark 4, we can write the displacement-based formulation of (7) as: find  $\mathbf{u}_h \in \mathbf{V}_h^B$  such that

$$\int_{\Omega} \left( \mathbf{F}^{-T}(\mathbf{u}_h)p_h + G(\mathbf{u}_h) \right) : \nabla \mathbf{v}_h \, d\mathbf{x} = \int_{\Omega} \mathbf{f} \cdot \mathbf{v}_h \, d\mathbf{x} + \int_{\Gamma_N} \mathbf{g}_N \cdot \mathbf{v}_h \, d\sigma, \quad \mathbf{v}_h \in \mathbf{V}_h^B, \quad (12)$$

where  $p_h = \lambda Q_h(U'(J(\mathbf{u}_h))J(\mathbf{u}_h))$ . Our numerical realization in the next section is based on (12).

Here we briefly discuss the issue of implementation of the scheme for a nearly incompressible elasticity problem, and also outline how to arrive at the displacement-based formulation. An easy way to implement the scheme is in the framework of a saddle point problem as in the case of mini-element. In this case, we linearize the whole saddle point system (7). Let  $\{\phi_1, \dots, \phi_M\}$  and  $\{\mu_1, \dots, \mu_N\}$  be finite element bases of  $\mathbf{V}_h$  and  $M_h$ , respectively, and  $\mathbf{u}_h = \sum_{k=1}^M u_k \phi_k$  and  $p_h = \sum_{k=1}^N p_k \phi_k$ . Assume that  $w = (u_1, \dots, u_M, p_1, \dots, p_N)^T$  be the nodal solution vector for both variables. We define

$$\begin{aligned} a(w, \mathbf{v}_h) &:= \int_{\Omega} \left( \mathbf{F}^{-T}(\mathbf{u}_h)p_h + G(\mathbf{u}_h) \right) : \nabla \mathbf{v}_h \, d\mathbf{x} - \int_{\Omega} \mathbf{f} \cdot \mathbf{v}_h \, d\mathbf{x} - \int_{\Gamma_N} \mathbf{g}_N \cdot \mathbf{v}_h \, d\sigma, \\ b(w, q_h) &:= \int_{\Omega} (p_h - \lambda U'(J(\mathbf{u}_h))J(\mathbf{u}_h))q_h \, d\mathbf{x}, \text{ and } F(w) := (F_1(w), F_2(w))^T, \end{aligned}$$

where

$$F_1(w) := \begin{pmatrix} a(w, \phi_1) \\ \vdots \\ a(w, \phi_M) \end{pmatrix}, \quad F_2(w) := \begin{pmatrix} b(w, \mu_1) \\ \vdots \\ b(w, \mu_N) \end{pmatrix}.$$

We apply the Newton method to solve this nonlinear system. First, we initialize the solution vector  $w_0$  satisfying the given Dirichlet boundary conditions. Then, we iterate until convergence with

$$J_k \Delta w_k = F(w_k),$$

where  $\Delta w_k := w_k - w_{k+1}$ , and  $J_k$  is the Jacobian of  $F$  evaluated at  $w_k$ . Since we work with a biorthogonal system, the pressure mass matrix in Jacobian  $J_k$  is diagonal. Hence the degree of freedom corresponding to the pressure in the linearized matrix is condensed out from the system just by inverting a diagonal matrix. However, the Jacobian after static condensation is non-symmetric.

An alternative to the implementation in the framework of the saddle point problem is to eliminate the pressure directly in the assembling process as is done for the nodal pressure formulation in [1]. Using the biorthogonality relation (6), the second equation of (7) yields  $p_h = \sum_{i=1}^N p_i \phi_i$  with

$$p_i = \frac{\lambda}{c_i} \int_{S_i} U'(J(\mathbf{u}_h))J(\mathbf{u}_h) \mu_i \, dx.$$

Then we substitute the pressure  $p_h$  in the equation (12) and linearize the system (12). In this case, it is necessary to integrate  $U'(J(\mathbf{u}_h))J(\mathbf{u}_h)\mu_i$  over  $S_i$  for which a neighboring search algorithm is necessary to find all elements  $T \subset S_i$ .

#### 4. Numerical results

In this section, we present some numerical examples using the above formulation in two and three dimensional elasticity. The examples considered in two and three dimensions are based on simplicial triangulation. We assume plane strain in the two-dimensional case. Comparing the numerical results produced by our new formulation (dual) with the one obtained by using the standard displacement formulation (standard) and mini-element (mini), we show that our new formulation does not lock in the nearly incompressible regime. That means we get a uniform convergence of the finite element solution when the Lamé parameter  $\lambda$  becomes very large or the Poisson ratio  $\nu$  approaches close to 0.5. We recall that Lamé parameters  $\lambda$  and  $\mu$  are related to Young's modulus  $E$  and Poisson ratio  $\nu$  by

$$\lambda = \frac{E\nu}{(1+\nu)(1-2\nu)}, \quad \text{and} \quad \mu = \frac{E}{2(1+\nu)}. \quad (13)$$

##### 4.1. Example-I (Cook's membrane example)

In this popular benchmark example [2, 11, 45], we consider a two-dimensional tapered panel

$$\Omega := \text{conv}\{(0, 0), (48, 44), (48, 60), (0, 44)\},$$

where  $\text{conv}\{\xi\}$  represents the convex hull of the set  $\xi$ . The left boundary of the panel is clamped in both directions and the right boundary is subjected to an in-plane shear load in the positive  $y$ - direction as shown in the left picture of Figure 1. Finite element analysis is performed using the initial mesh given in the left picture of Figure 1. In two right pictures of Figure 1, we show the vertical tip displacement at  $T$  with respect to the number of elements per edge for different finite element formulations using Poisson ratio  $\nu = 0.4999$ . The middle and right pictures show the cases of neo-Hookean and Mooney–Rivlin material model ( $c_m = 0.25$ ), respectively. We can see the extreme locking of the standard displacement formulation, whereas all other formulations show a very good convergence. Moreover, the vertical tip displacement at  $T$  with respect to the number of elements per edge using Poisson ratio  $\nu = 0.499999$  for both mixed formulations and both material models are given in two pictures of Figure 2. We can see the good convergence property of both mixed formulations here as well.

The mixed finite element scheme satisfies the stability property [27, 31] for linear elasticity and hence does not show any spurious pressure modes in this case. However, this does not necessarily guarantee the stability in the nonlinear regime. The pressure computed according to (8) is given in two pictures of Figure 3 for both material laws, where we do not have any spurious pressure modes. The pressure is computed using  $E = 250$  and  $\nu = 0.4999$ . As pressure is computed according to (8), where  $Q_h$  acts as an averaging operator, there will not be any spurious oscillation of the pressure.

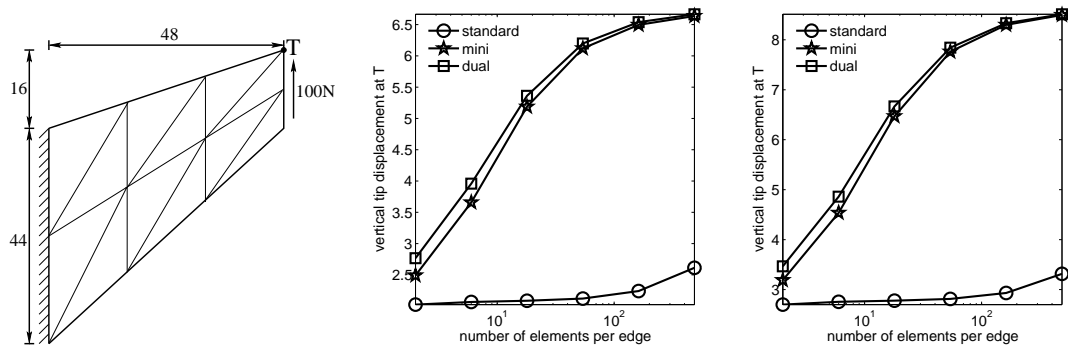


Figure 1. Problem setting and initial mesh (left), vertical tip displacement at  $T$  versus number of elements per edge neo-Hookean (middle) and Mooney–Rivlin (right),  $\nu = 0.4999$

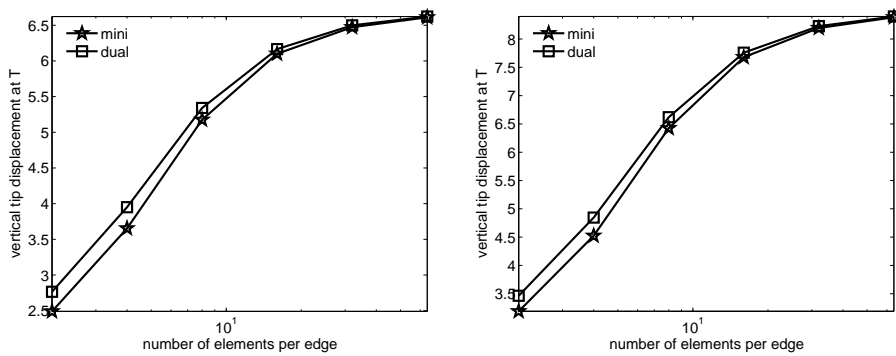


Figure 2. Vertical tip displacement at  $T$  versus number of elements per edge neo-Hookean (left) and Mooney–Rivlin (right),  $\nu = 0.499999$

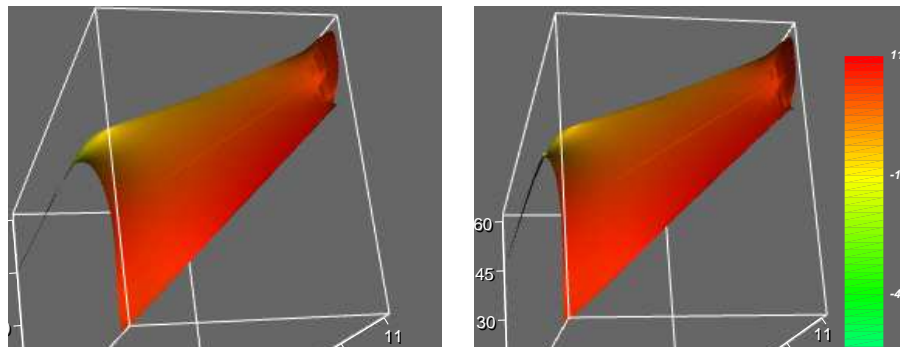


Figure 3. The computed pressure for neo-Hookean (left) and Mooney–Rivlin (right) material law.

#### 4.2. Example-II (Arch subjected to bending load)

In this numerical example, the formulation is tested for bending condition. The fixed circular arch beam with  $\theta_r=60^\circ$ ,  $t = 0.1m$  and  $r = 1m$  is considered as shown in Figure 4. The beam is subjected to a uniformly distributed load  $P = 20N/m$  in radial direction on the upper boundary in a range of the angle  $\theta_p=10^\circ$ . Quasi-static finite element analysis is performed where the load is applied in incremental steps. Vertical displacements at the point A are given in Table I using material parameters  $E = 250N/m^2$  and different values of Poisson's ratio  $\nu$ , where we use a mesh consisting of  $5 \times 40 \times 2$  elements. That means 5 elements on the breadth of the arch and 40 elements on the length of the arch resulting in the total of 400 elements, see the deformation of the grid on the right picture of Figure 4. We also tabulate the vertical displacements at point A using Poisson ratio  $\nu = 0.49999$  for different meshes in Table II, where  $m \times n \times 2$  means that  $m$  and  $n$  elements are used in the breadth and length of the arch, respectively. This shows that the finite element solution converges uniformly with respect to the mesh refinement.

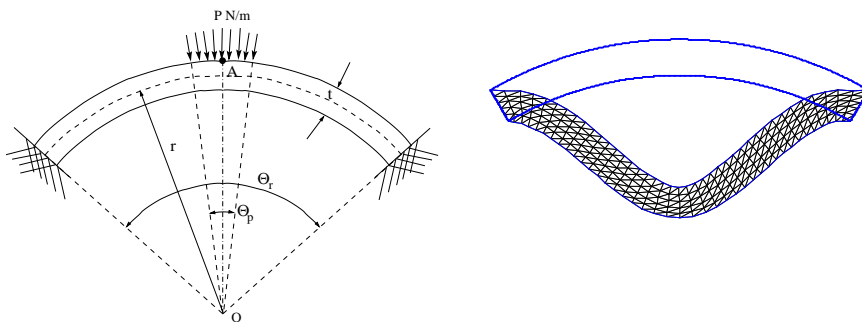


Figure 4. Problem setting and deformed mesh (circular arch)

The deflected finite element mesh obtained for  $\nu = 0.4999$  using the mixed formulation with neo-Hookean material model is shown in the right picture of Figure 4. Load-deflection curves using neo-Hookean and Mooney–Rivlin ( $c_m = 0.15$ ) material law for the Poisson's ratio  $\nu = 0.4999$  are compared in Figure 5. In both pictures, we can hardly see any difference among the two mixed formulations with continuous and discontinuous pressure.

#### 4.3. Example-III (Nearly incompressible block under compression)

In this example, we want to test the performance of our formulation for a nearly incompressible block under compression, see also [46]. Taking advantage of the symmetry of the problem, only one quarter of the block is modeled. The nodes on the top of the block are constrained in  $x$ - and  $y$ -directions. The load of  $320N/mm^2$  is applied as a uniformly distributed force on the

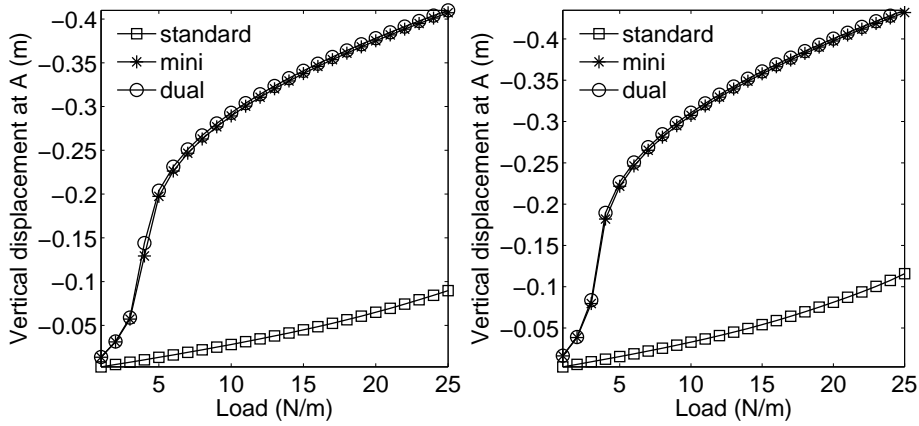


Figure 5. Load-deflection curves for circular arch, neo-Hookean material (left) and Mooney–Rivlin material ( $c_m = 0.15$ ) (right)

upper surface of the block on the area  $x \leq 0.5$  and  $y \leq 0.5$  as shown in the left picture of Figure 6. The material parameters are taken to be  $E = 240.5659612$  and  $\nu = 0.4999$ .

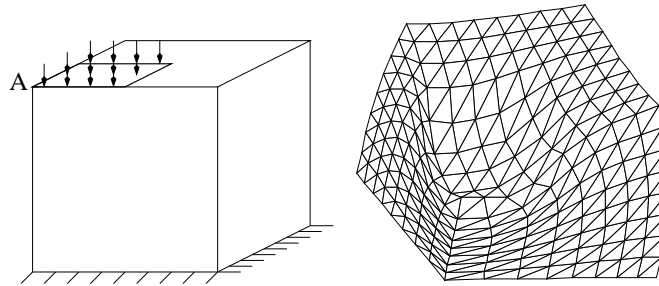


Figure 6. Problem setting (left), deformed configuration (right)

Finite element analysis is performed using a few quasi-static steps with an equal load increment in each step resulting in a total load of  $P_0 = 320N/mm^2$ . In some levels of refinement, it is even possible to get convergence in one quasi-static step. We note that the convergence of the Newton method is generally observed to be very fast using these nonlinear mixed formulations. Furthermore, it is possible to use large load resulting in the use of a few quasi-static steps compared to other displacement-based formulation, see [46, 16].

The numerical solution at  $A$  along the  $z$ -direction using neo-Hookean and Mooney–Rivlin material law are given in Tables III using different Poisson ratio  $\nu$ . We can see the robustness of our formulation that it does not show any sign of locking when Poisson ratio  $\nu$  reaches near to 0.5. We have shown the convergence of the vertical displacement at  $A$  in two pictures of Figure 7 in different levels of mesh refinement, where the initial level has 48 tetrahedra using  $\nu = 0.4999$ . We can see that the discrete solutions provided by our mixed formulations are very close to the finite element solutions provided by quadratic finite elements.

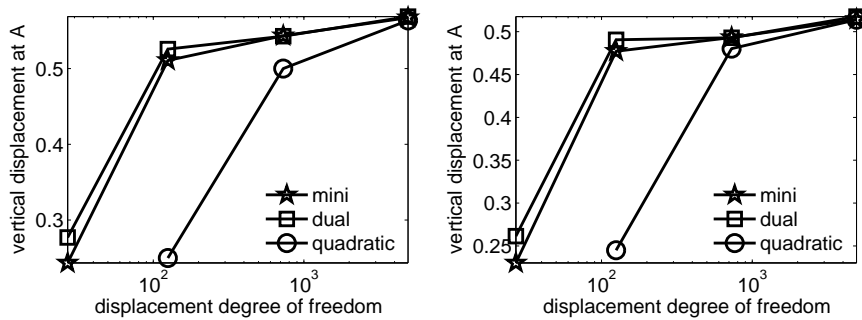


Figure 7. Vertical displacement at  $A$  versus number of degree of freedom, neo-Hookean (left) and Mooney–Rivlin ( $c_m = 0.2$ )(right)

## 5. Conclusion

We have proposed a mixed finite element method for nonlinear and nearly incompressible elasticity, where the pressure equation is discretized by using a Petrov–Galerkin formulation. Working with a biorthogonal system for the discretization of the pressure equation, the pressure variable is eliminated from the system and we arrive at a displacement–based formulation for which an efficient iterative solver can be used. As the discrete formulation provides a stable approach for linear elasticity, the numerical results in the nonlinear case are also quite promising. However, more numerical experiments are necessary to test the performance of our mixed formulation for the general hyperelastic and other nonlinear models in elasticity.

## REFERENCES

1. Bonet J, Burton AJ. A simple average nodal pressure tetrahedral element for incompressible and nearly incompressible dynamic explicit applications. *Communications in Numerical Methods in Engineering* 1998; **14**:437–449.
2. Simo J, Rifai M. A class of assumed strain method and the methods of incompatible modes. *International Journal for Numerical Methods in Engineering* 1990; **29**:1595–1638.
3. Simo J, Armero F. Geometrically nonlinear enhanced strain mixed methods and the method of incompatible modes. *International Journal for Numerical Methods in Engineering* 1992; **33**:1413–1449.
4. Glaser S, Armero F. On the formulation of enhanced strain finite elements in finite deformation. *Engineering Computations* 1997; **14**:759–791.
5. Armero F. On the locking and stability of finite elements in finite deformation plane strain problems. *Computers and Structures* 2000; **75**:261–290.
6. Reddy B, Simo J. Stability and convergence of a class of enhanced strain methods. *SIAM Journal on Numerical Analysis* 1995; **32**:1705–1728.
7. Braess D, Carstensen C, Reddy B. Uniform convergence and a posteriori error estimators for the enhanced strain finite element method. *Numerische Mathematik* 2004; **96**:461–479.
8. Lamichhane B, Reddy B, Wohlmuth B. Convergence in the incompressible limit of finite element approximations based on the Hu–Washizu formulation. *Numerische Mathematik* 2006; **104**:151–175.
9. Hu H. On some variational principles in the theory of elasticity and the theory of plasticity. *Scientia Sinica* 1955; **4**:33–54.
10. Washizu K. *Variational methods in elasticity and plasticity*. 3rd edn., Pergamon Press, 1982.
11. Kasper E, Taylor R. A mixed-enhanced strain method. Part I: geometrically linear problems. *Computers and Structures* 2000; **75**:237–250.
12. Kasper E, Taylor R. A mixed-enhanced strain method. Part II: geometrically nonlinear problems. *Computers and Structures* 2000; **75**:251–260.

13. Taylor R. A mixed-enhanced formulation for tetrahedral finite elements. *International Journal for Numerical Methods in Engineering* 2000; **47**:205–227.
14. Nagtegaal J, Parks D, Rice J. On numerically accurate finite element solutions in the fully plastic range. *Computer Methods in Applied Mechanics and Engineering* 1974; **4**:153–177.
15. Simo J, Taylor R, Pister K. Variational and projection methods for the volume constraint in finite deformation elasto-plasticity. *Computer Methods in Applied Mechanics and Engineering* 1985; **51**:177–208.
16. Chavan K, Lamichhane B, Wohlmuth B. Locking-free finite element methods for linear and nonlinear elasticity in 2D and 3D. *Computer Methods in Applied Mechanics and Engineering* 2007; **196**:4075–4086.
17. Brezzi F, Fortin M. *Mixed and hybrid finite element methods*. Springer-Verlag, New York, 1991.
18. Braess D. *Finite Elements. Theory, fast solver, and applications in solid mechanics*. Cambridge University Press, Second Edition, 2001.
19. Hughes T. *The finite element method: Linear, static and dynamic finite element analysis*. Prentice-Hall, 1987.
20. Guo Y, Ortiz M, Belytschko T, Repetto EA. Triangular composite finite elements. *International Journal for Numerical Methods in Engineering* 2000; **47**:287–316.
21. Dohrmann C, Heinstein M, Jung J, Key S, Witkowski W. Node-based uniform strain elements for three-node triangular and four-node tetrahedral meshes. *International Journal for Numerical Methods in Engineering* 2000; **47**:1549–1568.
22. Bonet J, Marriott H, Hassan O. Stability and comparison of different linear tetrahedral formulations for nearly incompressible explicit dynamic applications. *International Journal for Numerical Methods in Engineering* 2001; **50**:119–133.
23. Pires FMA, de Souza Neto EA, de la Cuesta Padilla JL. An assessment of the average nodal volume formulation for the analysis of nearly incompressible solids under finite strains. *Communications in Numerical Methods in Engineering* 2004; **20**:569–583.
24. de Souza Neto EA, Pires FMA, Owen DRJ. F-bar-based linear triangles and tetrahedra for finite strain analysis of nearly incompressible solids. part I: formulation and benchmarking. *International Journal for Numerical Methods in Engineering* 2005; **62**:353–383.
25. Bank R, Rose D. Some error estimates for the box method. *SIAM Journal on Numerical Analysis* 1987; **24**:777–787.
26. Ewing RE, Lin T, Lin Y. On the accuracy of the finite volume element method based on piecewise linear polynomials. *SIAM Journal on Numerical Analysis* 2002; **39**:1865–1888.
27. Lamichhane B. Inf-sup stable finite element pairs based on dual meshes and bases for nearly incompressible elasticity. *IMA Journal of Numerical Analysis* 2008; Published online.
28. Stein E, Rter M. Finite element methods for elasticity with error-controlled discretization and model adaptivity. *Encyclopedia of Computational Mechanics*, Stein E, de Borst R, Hughes T (eds.). Wiley, 2004; 5–58.
29. Ecker A, Zulehner W. On the smoothing property of multigrid methods in the non-symmetric case. *Numerical Linear Algebra with Applications* 1996; **3**:161–172.
30. Saad Y. *Iterative Methods for Sparse Linear Systems*. Society for Industrial and Applied Mathematics, Philadelphia, USA, Second Edition, 2003.
31. Lamichhane B. A mixed finite element method based on a biorthogonal system for nearly incompressible elastic problems. *Proceedings of the 14th Biennial Computational Techniques and Applications Conference, CTAC-2008, ANZIAM J.*, vol. 50, Mercer GN, Roberts AJ (eds.), 2008; C324–C338.
32. Kim C, Lazarov R, Pasciak J, Vassilevski P. Multiplier spaces for the mortar finite element method in three dimensions. *SIAM Journal on Numerical Analysis* 2001; **39**:519–538.
33. Bai W. A quadrilateral ‘mini’ finite element for the Stokes problem. *Computer Methods in Applied Mechanics and Engineering* 1997; **143**:41–47.
34. Ciarlet P. *Mathematical Elasticity Volume I: Three-Dimensional Elasticity*. North-Holland: Amsterdam, 1988.
35. Adams R. *Sobolev Spaces*. Academic Press New York, 1975.
36. Braess D, Ming PB. A finite element method for nearly incompressible elasticity problems. *Mathematics of Computation* 2005; **74**:25–52.
37. Girault V, Raviart PA. *Finite Element Methods for Navier-Stokes Equations*. Springer-Verlag: Berlin, 1986.
38. Quarteroni A, Valli A. *Numerical approximation of partial differential equations*. Springer-Verlag: Berlin, 1994.
39. Arnold DN, Brezzi F, Fortin M. A stable finite element for the Stokes equations. *Calcolo* 1984; **21**:337–344.
40. Galántai A. *Projectors and Projection Methods*. Kluwer Academic Publishers: Dordrecht, 2003.
41. Szyld D. The many proofs of an identity on the norm of oblique projections. *Numerical Algorithms* 2006; **42**:309–323.

42. Scott L, Zhang S. Finite element interpolation of nonsmooth functions satisfying boundary conditions. *Mathematics of Computation* 1990; **54**:483–493.
43. Bernardi C, Maday Y, Patera A. Domain decomposition by the mortar element method. *Asymptotic and numerical methods for partial differential equations with critical parameters*, et al HK (ed.), Reidel, Dordrecht, 1993; 269–286.
44. Ciarlet P. *The finite element method for elliptic problems*. North Holland, Amsterdam, 1978.
45. Küssner M, Reddy B. The equivalent parallelogram and parallelepiped, and their application to stabilized finite elements in two and three dimensions. *Computer Methods in Applied Mechanics and Engineering* 2001; **190**:1967–1983.
46. Reese S, Wriggers P, Reddy B. A new locking-free brick element technique for large deformation problems in elasticity. *Computers and Structures* 2000; **75**:291–304.

Table I. Displacement at  $A$  for different Poisson ratio  $\nu$ , circular arch with neo-Hookean and Mooney–Rivlin material law

$\nu$	neo-Hooke		Mooney–Rivlin, $c_m = 0.15$	
	mini	dual	mini	dual
0.4900000	-0.408414	-0.410871	-0.433024	-0.435334
0.4990000	-0.407266	-0.410063	-0.432145	-0.434768
0.4999000	-0.407136	-0.409973	-0.432044	-0.434704
0.4999900	-0.407123	-0.409964	-0.432033	-0.434697
0.4999990	-0.407156	-0.409976	-0.432067	-0.43471
0.4999999	-0.407156	-0.409976	-0.432066	-0.43471

Table II. Displacement at  $A$  for different meshes, circular arch with neo-Hookean and Mooney–Rivlin material law

mesh	neo-Hooke		Mooney–Rivlin, $c_m = 0.15$	
	mini	dual	mini	dual
$3 \times 20 \times 2$	-0.391958	-0.399527	-0.417585	-0.424577
$5 \times 40 \times 2$	-0.407123	-0.409964	-0.432033	-0.434697
$8 \times 80 \times 2$	-0.424976	-0.426185	-0.450797	-0.451897

Table III. Displacement at  $A$  for different Poisson ratio  $\nu$  for the nearly incompressible block

$\nu$	neo-Hooke		Mooney–Rivlin, $c_m = 0.2$	
	mini	dual	mini	dual
0.4900000	-0.553276	-0.552955	-0.503553	-0.502763
0.4990000	-0.546155	-0.546436	-0.494267	-0.493915
0.4999000	-0.545365	-0.545741	-0.493260	-0.492987
0.4999900	-0.545285	-0.545671	-0.493159	-0.492894
0.4999990	-0.545277	-0.545664	-0.493148	-0.492884
0.4999999	-0.545276	-0.545663	-0.493147	-0.492883